



A meshless method for the numerical solution of the Cauchy problem associated with three-dimensional Helmholtz-type equations

Liviu Marin

School of the Environment, University of Leeds, Woodhouse Lane, Leeds LS2 9JT, UK

Abstract

In this paper, the application of the method of fundamental solutions to the Cauchy problem associated with three-dimensional Helmholtz-type equations is investigated. The resulting system of linear algebraic equations is ill-conditioned and therefore its solution is regularized by employing the zeroth-order Tikhonov functional, while the choice of the regularization parameter is based on the L-curve method. Numerical results are presented for under-, equally- and over-determined Cauchy problems in a piecewise smooth geometry. The convergence, accuracy and stability of the method with respect to increasing the number of source points and the distance between the source points and the boundary of the solution domain, and decreasing the amount of noise added into the input data, respectively, are analysed.

© 2004 Elsevier Inc. All rights reserved.

Keywords: Meshless method; Method of fundamental solutions; Cauchy problem; Helmholtz-type equations; Regularization; Inverse problem

E-mail address: liviu@env.leeds.ac.uk

1. Introduction

The method of fundamental solutions (MFS) was originally introduced by Kupradze and Aleksidze [1], whilst its numerical formulation was first given by Mathon and Johnston [2]. The main idea of the MFS consists of approximating the solution of the problem by a linear combination of fundamental solutions with respect to some singularities/source points which are located outside the domain. Then the original problem is reduced to determining the unknown coefficients of the fundamental solutions and the coordinates of the source points by requiring the approximation to satisfy the boundary conditions and hence solving a nonlinear problem. If the source points are a priori fixed then the coefficients of the MFS approximation are determined by solving a linear problem. An excellent survey of the MFS and related methods over the past three decades has been presented by Fairweather and Karageorghis [3]. The advantages of the MFS over domain discretisation methods, such as the finite-difference (FDM) and the finite element methods (FEM), are very well documented, see e.g. Fairweather and Karageorghis [3]. In addition, the MFS has all the advantages of boundary methods, such as the boundary element method (BEM), as well as several advantages over other boundary methods. For example, the MFS does not require an elaborate discretisation of the boundary, integrations over the boundary are avoided, the solution in the interior of the domain is evaluated without extra quadratures, its implementation is very easy and only little data preparation is required. The most arguable issue regarding the MFS is still the location of the source points. However, this problem can be overcome by employing a nonlinear least-squares minimisation procedure. Alternatively, the source points can be prescribed a priori, see [4–6], and the post-processing analysis of the errors can indicate their optimal location. The MFS has been successfully applied to solving a wide variety of boundary value problems. Karageorghis and Fairweather [7] have solved numerically the biharmonic equation using the MFS and later their method has been modified in order to take into account the presence of boundary singularities in both the Laplace and the biharmonic equations by Poullikkas et al. [8]. Furthermore, Poullikkas et al. [9] have investigated the numerical solutions of the inhomogeneous harmonic and biharmonic equations by reducing these problems to the homogeneous corresponding cases and subtracting a particular solution of the governing equation. The MFS has been formulated for three-dimensional Signorini boundary value problems and it has been tested on a three-dimensional electropainting problem related to the coating of vehicle roofs in Poullikkas et al. [10]. Whilst Karageorghis and Fairweather [11] have studied the use of the MFS for the approximate solution of three-dimensional isotropic materials with axisymmetrical geometry and both axisymmetrical and arbitrary boundary conditions. The application of the MFS to two-dimensional problems of steady-state heat conduction and elastostatics in isotropic

and anisotropic bimetals has been addressed by Berger and Karageorghis [12,13]. Karageorghis [14] has investigated the calculation of the eigenvalues of the Helmholtz equation subject to homogeneous Dirichlet boundary conditions for circular and rectangular geometries by employing the MFS, whilst Poullikkas et al. [15] have successfully applied the MFS for solving three-dimensional elastostatics problems. The MFS, in conjunction with singular value decomposition, has been employed by Ramachandran [16] in order to obtain numerical solutions of the Laplace and the Helmholtz equations. Recently, Balakrishnan et al. [17] have proposed an operator splitting-radial basis function method as a generic solution procedure for transient nonlinear Poisson problems by combining the concepts of operator splitting, radial basis function interpolation, particular solutions and the MFS.

Helmholtz-type equations arise naturally in many physical applications related to wave propagation and vibration phenomena. It is often used to describe the vibration of a structure [18], the acoustic cavity problem [19], the radiation wave [20] and the scattering of a wave [21]. The knowledge of the Dirichlet, Neumann or mixed boundary conditions on the entire boundary of the solution domain gives rise to direct problems for Helmholtz-type equations which have been extensively studied in the literature, see for example [22–24]. Unfortunately, many engineering problems do not belong to this category. In particular, the boundary conditions are often incomplete, either in the form of underspecified and overspecified boundary conditions on different parts of the boundary or the solution is prescribed at some internal points in the domain. These are inverse problems, and it is well known that they are generally ill-posed, i.e. the existence, uniqueness and stability of their solutions are not always guaranteed, see e.g. Hadamard [25].

A classical example of an inverse problem for Helmholtz-type equations is the Cauchy problem in which boundary conditions for both the solution and its normal derivative are prescribed only on a part of the boundary of the solution domain, whilst no information is available on the remaining part of the boundary. Unlike in direct problems, the uniqueness of the Cauchy problem is guaranteed without the necessity of removing the eigenvalues for the Laplacian. A BEM-based acoustic holography technique using the singular value decomposition (SVD) for the reconstruction of sound fields generated by irregularly shaped sources has been developed by Bai [26]. The vibrational velocity, sound pressure and acoustic power on the vibrating boundary comprising an enclosed space have been reconstructed by Kim and Ih [27] who have used the SVD in order to obtain the inverse solution in the least-squares sense and to express the acoustic modal expansion between the measurement and source field. Wang and Wu [28] have developed a method employing the spherical wave expansion theory and a least-squares minimisation to reconstruct the acoustic pressure field from a vibrating object and their method has been extended to the reconstruction of acoustic pressure fields inside the cavity of a

vibrating object by Wu and Yu [29]. DeLillo et al. [30] have detected the source of acoustical noise inside the cabin of a midsize aircraft from measurements of the acoustical pressure field inside the cabin by solving a linear Fredholm integral equation of the first kind in two-dimensions and recently they have extended this study to three-dimensional problems, see DeLillo et al. [31]. Marin et al. [32,33] have solved the Cauchy problem for Helmholtz-type equations by employing the BEM in conjunction with an alternating iterative algorithm and the conjugate gradient method, respectively.

To our knowledge, the application of the MFS to the Cauchy problem associated with three-dimensional Helmholtz-type equations has not been investigated yet. The MFS discretised system of equations is ill-conditioned and hence it is solved by employing the zeroth-order Tikhonov regularization method, see e.g. Tikhonov and Arsenin [34], whilst the choice of the regularization parameter is based on the L-curve criterion, see Hansen [35]. Three examples for under-, equally- and over-determined Cauchy problems associated with the three-dimensional Helmholtz and modified Helmholtz equations in a piecewise smooth geometry are investigated. In addition, the convergence, accuracy and stability of the method with respect to the location and the number of source points and the amount of noise added into the Cauchy input data, respectively, are analysed.

2. Mathematical formulation

Consider an open bounded domain $\Omega \subset \mathbb{R}^3$ and assume that Ω is bounded by a piecewise smooth boundary $\Gamma \equiv \partial\Omega$, such that $\Gamma = \Gamma_1 \cup \Gamma_2$, where $\Gamma_1, \Gamma_2 \neq \emptyset$ and $\Gamma_1 \cap \Gamma_2 = \emptyset$. Referring to acoustics for the sake of the physical explanation, we assume that the acoustical field $u(\mathbf{x})$ satisfies the Helmholtz-type equation in the domain Ω , namely

$$\mathcal{L}u(\mathbf{x}) \equiv (\Delta \pm k^2)u(\mathbf{x}) = 0, \quad \mathbf{x} \in \Omega, \quad (1)$$

where $k \in \mathbb{R}$ is the frequency of the acoustical field u . Let $\mathbf{n}(\mathbf{x})$ be the outward unit normal vector at Γ and $v(\mathbf{x}) \equiv (\nabla u \cdot \mathbf{n})(\mathbf{x})$ be the normal velocity of the sound at a point $\mathbf{x} \in \Gamma$. In the direct problem formulation, the knowledge of the acoustical field and/or normal velocity of the sound on the whole boundary Γ gives the corresponding Dirichlet, Neumann, or mixed boundary conditions which enables us to determine the acoustical field in the domain Ω . If it is possible to measure both the acoustical field and the normal velocity of the sound on a part of the boundary Γ , say Γ_1 , then this leads to the mathematical formulation of an inverse problem consisting of Eq. (1) and the boundary conditions

$$u(\mathbf{x}) = \tilde{u}(\mathbf{x}), \quad v(\mathbf{x}) = \tilde{v}(\mathbf{x}), \quad \mathbf{x} \in \Gamma_1, \quad (2)$$

where \tilde{u} and \tilde{v} are prescribed functions and $\Gamma_1 \subset \Gamma$, $\text{meas}(\Gamma_1) > 0$. In the above formulation of the boundary conditions (2), it can be seen that the boundary Γ_1 is overspecified by prescribing both the acoustical field $u|_{\Gamma_1}$ and the normal velocity of the sound $v|_{\Gamma_1}$, whilst the boundary Γ_2 is underspecified since both the acoustical field $u|_{\Gamma_2}$ and the normal velocity of the sound $v|_{\Gamma_2}$ are unknown and have to be determined. It should be noted that the problem studied in this paper is of practical importance.

This problem, termed the Cauchy problem, is much more difficult to solve both analytically and numerically than the direct problem, since the solution does not satisfy the general conditions of well-posedness. Whilst the Dirichlet, Neumann or mixed direct problems associated to Eq. (1) do not always have a unique solution due to the eigensolutions, see Chen and Zhou [36], the solution of the Cauchy problem given by Eqs. (1) and (2) is unique based on the analytical continuation property. However, it is well known that if this solution exists then it is unstable with respect to small perturbations in the data on Γ_2 , see e.g. Hadamard [25]. Thus the problem under investigation is ill-posed and we cannot use a direct approach, such as the Gauss elimination method, in order to solve the system of linear equations which arises from the discretisation of the partial differential equations (1) and the boundary conditions (2). Therefore, regularization methods are required in order to solve accurately the Cauchy problem associated with Helmholtz-type equations.

3. Method of fundamental solutions

The fundamental solutions \mathcal{F}_H and \mathcal{F}_{MH} of the Helmholtz ($\mathcal{L} \equiv \Delta + k^2$) and the modified Helmholtz ($\mathcal{L} \equiv \Delta - k^2$) equations (1), respectively, in the three-dimensional case are given by, see e.g. Fairweather and Karageorghis [3],

$$\mathcal{F}_H(\mathbf{x}, \mathbf{y}) = \frac{1}{4\pi r(\mathbf{x}, \mathbf{y})} \exp(-ikr(\mathbf{x}, \mathbf{y})), \quad \mathbf{x} \in \bar{\Omega}, \quad \mathbf{y} \in \mathbb{R}^3 \setminus \bar{\Omega}, \tag{3}$$

$$\mathcal{F}_{MH}(\mathbf{x}, \mathbf{y}) = \frac{1}{4\pi r(\mathbf{x}, \mathbf{y})} \exp(-kr(\mathbf{x}, \mathbf{y})), \quad \mathbf{x} \in \bar{\Omega}, \quad \mathbf{y} \in \mathbb{R}^3 \setminus \bar{\Omega}, \tag{4}$$

where $r(\mathbf{x}, \mathbf{y}) = \sqrt{(x_1 - y_1)^2 + (x_2 - y_2)^2 + (x_3 - y_3)^2}$ represents the distance between the domain point $\mathbf{x} = (x_1, x_2, x_3)$ and the source point $\mathbf{y} = (y_1, y_2, y_3)$.

The main idea of the MFS consists of the approximation of the acoustical field in the solution domain by a linear combination of fundamental solutions with respect to M source points \mathbf{y}_j in the form

$$u(\mathbf{x}) \approx u^M(\mathbf{a}, \mathbf{Y}; \mathbf{x}) = \sum_{j=1}^M a_j \mathcal{F}(\mathbf{x}, \mathbf{y}^j), \quad \mathbf{x} \in \bar{\Omega}, \tag{5}$$

where $\mathcal{F} = \mathcal{F}_H$ in the case of the Helmholtz equation, $\mathcal{F} = \mathcal{F}_{MH}$ in the case of the modified Helmholtz equation, $\mathbf{a} = (a_1, \dots, a_M)$ and \mathbf{Y} is a $3M$ -vector containing the coordinates of the source points $\mathbf{y}^j, j = 1, \dots, M$. Then the normal velocity of the sound can be approximated on the boundary Γ by

$$v(\mathbf{x}) \approx v^M(\mathbf{a}, \mathbf{Y}, \mathbf{n}; \mathbf{x}) = \sum_{j=1}^M a_j \mathcal{G}(\mathbf{x}, \mathbf{y}^j; \mathbf{n}), \quad \mathbf{x} \in \Gamma, \tag{6}$$

where $\mathcal{G}(\mathbf{x}, \mathbf{y}; \mathbf{n}) = \nabla_{\mathbf{x}} \mathcal{F}(\mathbf{x}, \mathbf{y}) \cdot \mathbf{n}(\mathbf{x})$ and \mathcal{G}_H in the case of the Helmholtz equation and \mathcal{G}_{MH} in the case of the modified Helmholtz equation are given by

$$\mathcal{G}_H(\mathbf{x}, \mathbf{y}; \mathbf{n}) = -\frac{(\mathbf{x} - \mathbf{y}) \cdot \mathbf{n}(\mathbf{x})}{r(\mathbf{x}, \mathbf{y})} \left(ik + \frac{1}{r(\mathbf{x}, \mathbf{y})} \right) \mathcal{F}_H(\mathbf{x}, \mathbf{y}), \quad \mathbf{x} \in \Gamma, \quad \mathbf{y} \in \mathbb{R}^3 \setminus \overline{\Omega}, \tag{7}$$

$$\mathcal{G}_{MH}(\mathbf{x}, \mathbf{y}; \mathbf{n}) = -\frac{(\mathbf{x} - \mathbf{y}) \cdot \mathbf{n}(\mathbf{x})}{r(\mathbf{x}, \mathbf{y})} \left(k + \frac{1}{r(\mathbf{x}, \mathbf{y})} \right) \mathcal{F}_{MH}(\mathbf{x}, \mathbf{y}), \quad \mathbf{x} \in \Gamma, \quad \mathbf{y} \in \mathbb{R}^3 \setminus \overline{\Omega}. \tag{8}$$

If N collocation points $\mathbf{x}^i, i = 1, \dots, N$, are chosen on the overspecified boundary Γ_1 and the location of the source points $\mathbf{y}^j, j = 1, \dots, M$, is set then Eqs. (5) and (6) recast as a system of $2N$ linear algebraic equations with M unknowns which can be generically written as

$$\mathbb{A}\mathbf{X} = \mathbf{F}, \tag{9}$$

where the MFS matrix A , the unknown vector \mathbf{X} and the right-hand side vector \mathbf{F} are given by

$$\begin{aligned} A_{i,j} &= \mathcal{F}(\mathbf{x}^i, \mathbf{y}^j), \quad A_{N+i,j} = \mathcal{G}(\mathbf{x}^i, \mathbf{y}^j), \quad X_j = a_j, \\ F_i &= u(\mathbf{x}^i), \quad F_{N+i} = v(\mathbf{x}^i), \quad i = 1, \dots, N, \quad j = 1, \dots, M. \end{aligned} \tag{10}$$

It should be noted that in order to uniquely determine the solution \mathbf{X} of the system of linear algebraic equations (9), i.e. the coefficients $a_j, j = 1, \dots, M$, in the approximations (5) and (6), the number N of boundary collocation points and the number M of source points must satisfy the inequality $M \leq 2N$. However, the system of linear algebraic equations (9) cannot be solved by direct methods, such as the least-squares method, since such an approach would produce a highly unstable solution due to the large value of the condition number of the matrix \mathbb{A} which increases dramatically as the number of boundary collocation points and source points increases. It should be mentioned that for inverse problems, the resulting systems of linear algebraic equations are ill-conditioned, even if other well-known numerical methods (FDM, FEM or BEM) are employed. Although the MFS system of linear algebraic equations (9) is ill-conditioned even when dealing with direct problems, the MFS has no longer this disadvantage in comparison with other numerical methods

and, in addition, it preserves its advantages, such as the lack of any mesh, the high accuracy of the numerical results, etc.

3.1. Tikhonov regularization method

Several regularization procedures have been developed to solve such ill-conditioned systems, see for example Hansen [37]. However, we only consider the Tikhonov regularization method, see Tikhonov and Arsenin [34], in our study since it is simple, non-iterative and it provides an explicit solution, see Eq. (13) below. Furthermore, the Tikhonov regularization method is feasible to apply for large systems of equations unlike the singular value decomposition which may become prohibitive for such large problems, see Hansen [35].

The Tikhonov regularized solution to the system of linear algebraic equations (9) is sought as

$$\mathbf{X}_\lambda : \mathcal{T}_\lambda(\mathbf{X}_\lambda) = \min_{\mathbf{X} \in \mathbb{R}^M} \mathcal{T}_\lambda(\mathbf{X}), \tag{11}$$

where \mathcal{T}_λ represents the s -th order Tikhonov functional given by

$$\mathcal{T}_\lambda(\cdot) : \mathbb{R}^M \rightarrow [0, \infty), \quad \mathcal{T}_\lambda(\mathbf{X}) = \|\mathbb{A}\mathbf{X} - \mathbf{F}\|_2^2 + \lambda^2 \|\mathbb{R}^{(s)}\mathbf{X}\|_2^2, \tag{12}$$

the matrix $\mathbb{R}^{(s)} \in \mathbb{R}^{(M-s) \times M}$ induces a \mathcal{C}^s -constraint on the solution \mathbf{X} and $\lambda > 0$ is the regularization parameter to be chosen. Formally, the Tikhonov regularized solution \mathbf{X}_λ of the problem (11) is given as the solution of the regularized equation

$$(\mathbb{A}^T \mathbb{A} + \lambda^2 \mathbb{R}^{(s)T} \mathbb{R}^{(s)})\mathbf{X} = \mathbb{A}^T \mathbf{F}. \tag{13}$$

Regularization is necessary when solving ill-conditioned systems of linear equations because the simple least-squares solution, i.e. $\lambda = 0$, is completely dominated by contributions from data errors and rounding errors. By adding regularization we are able to damp out these contributions and maintain the norm $\|\mathbb{R}^{(s)}\mathbf{X}\|_2$ to be of reasonable size.

3.2. Choice of the regularization parameter

The choice of the regularization parameter in equation (13) is crucial for obtaining a stable solution and this is discussed next. If too much regularization, or damping, i.e. λ^2 is large, is imposed on the solution then it will not fit the given data \mathbf{F} properly and the residual norm $\|\mathbb{A}\mathbf{X} - \mathbf{F}\|_2$ will be too large. If too little regularization is imposed on the solution, i.e. λ^2 is small, then the fit will be good, but the solution will be dominated by the contributions from the data errors, and hence $\|\mathbb{R}^{(s)}\mathbf{X}\|_2$ will be too large. It is quite natural to plot the norm of the solution as a function of the norm of the residual parametrised

by the regularization parameter λ , i.e. $\{\|\mathbb{A}\mathbf{X}_\lambda - \mathbf{F}\|_2, \|\mathbb{R}^{(s)}\mathbf{X}_\lambda\|_2, \lambda > 0\}$. Hence, the L-curve is really a trade-off curve between two quantities that both should be controlled and, according to the L-curve criterion, the optimal value λ_{opt} of the regularization parameter λ is chosen at the “corner” of the L-curve, see Hansen [35,37].

As with every practical method, the L-curve has its advantages and disadvantages. There are two main disadvantages or limitations of the L-curve criterion. The first disadvantage is concerned with the reconstruction of very smooth exact solutions, see Tikhonov et al. [38]. For such solutions, Hanke [39] showed that the L-curve criterion will fail, and the smoother the solution, the worse the regularization parameter λ computed by the L-curve criterion. However, it is not clear how often very smooth solutions arise in applications. The second limitation of the L-curve criterion is related to its asymptotic behaviour as the problem size M increases. As pointed out by Vogel [40], the regularization parameter λ computed by the L-curve criterion may not behave consistently with the optimal parameter λ_{opt} as M increases. However, this ideal situation in which the same problem is discretised for increasing M may not arise so often in practice. Often the problem size M is fixed by the particular measurement setup given by N , and if a larger M is required then a new experiment must be undertaken since the inequality $M \leq 2N$ must be satisfied. Apart from these two limitations, the advantages of the L-curve criterion are its robustness and ability to treat perturbations consisting of correlated noise, see for more details Hansen [35].

4. Numerical results and discussion

Although neither convergence nor estimate proofs are as yet available for the MFS, the numerical results presented in this section for the Cauchy problem associated with Helmholtz-type equations indicate that the proposed method is feasible and efficient. In order to present the performance of the MFS in conjunction with the zeroth-order Tikhonov regularization method, we solve under-, equally- and over-determined Cauchy problems (1) and (2) for two typical examples corresponding to the Helmholtz and modified Helmholtz equations in a piecewise smooth geometry, such as the cube $\Omega = (-0.5, 0.5)^3 \subset \mathbb{R}^3$, namely:

Example 1 (Helmholtz equation, i.e. $\mathcal{L} \equiv \Delta + k^2$). We consider the following analytical solutions for the acoustical field:

$$u^{(\text{an})}(\mathbf{x}) = \cos(\xi_1 x_1 + \xi_2 x_2 + \xi_3 x_3), \quad \mathbf{x} = (x_1, x_2, x_3) \in \Omega, \quad (14)$$

where $k = -3.0$, $\zeta_1 = 1.0$, $\zeta_2 = 2.0$ and $\zeta_3 = \sqrt{k^2 - \zeta_1^2 - \zeta_2^2} = 2.0$. Here $\Gamma_1 = \bigcup_{j=1}^J \Gamma^{(j)}$ and $\Gamma_2 = \Gamma \setminus \Gamma_1 = \bigcup_{j=J+1}^6 \Gamma^{(j)}$, $J \in \{1, 3, 5\}$, where $\Gamma = \bigcup_{j=1}^6 \Gamma^{(j)}$, $\Gamma^{(j)} = \{x \in \Gamma | x_j = -0.5\}$, $j = 1, 2, 3$, and $\Gamma^{(j+3)} = \{x \in \Gamma | x_j = 0.5\}$, $j = 1, 2, 3$.

Example 2 (Modified Helmholtz equation, i.e. $\mathcal{L} \equiv \Delta - k^2$). We consider the following analytical solutions for the acoustical field:

$$u^{(an)}(\mathbf{x}) = \exp(\zeta_1 x_1 + \zeta_2 x_2 + \zeta_3 x_3), \quad \mathbf{x} = (x_1, x_2, x_3) \in \Omega, \tag{15}$$

where $k = 2.0$, $\zeta_1 = 1.0$, $\zeta_2 = 0.5$ and $\zeta_3 = \sqrt{k^2 - \zeta_1^2 - \zeta_2^2}$. Here $\Gamma_1 = \bigcup_{j=1}^J \Gamma^{(j)}$ and $\Gamma_2 = \Gamma \setminus \Gamma_1 = \bigcup_{j=J+1}^6 \Gamma^{(j)}$, $J \in \{1, 3, 5\}$.

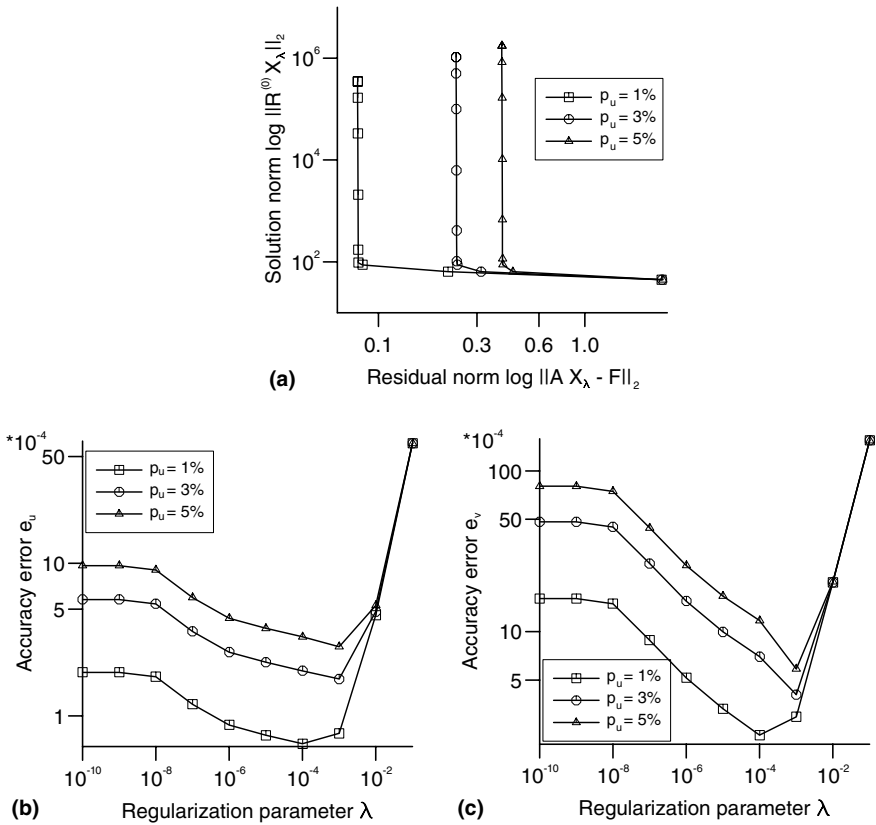


Fig. 1. (a) The L-curves, and the accuracy errors (b) e_u and (c) e_v , as functions of the regularization parameter λ , obtained for various levels of noise added into the acoustical field $u|_{\Gamma}$, namely $p_u = 1\%$ (\square), $p_u = 3\%$ (\circ) and $p_u = 5\%$ (\triangle), with $M = 150$ source points, $N = 100$ boundary collocation points and $R = 5.0$ for Example 1(iii).

It should be noted that for both examples considered, the Cauchy data is available on a portion Γ_1 of the boundary Γ such that (i) $\text{meas}(\Gamma_1)/5 = \text{meas}(\Gamma_2) = \text{meas}(\Gamma)/6$, (ii) $\text{meas}(\Gamma_1) = \text{meas}(\Gamma_2) = \text{meas}(\Gamma)/2$ and (iii) $\text{meas}(\Gamma_1) = \text{meas}(\Gamma_2)/5 = \text{meas}(\Gamma)/6$ corresponding to under-, equally- and over-determined Cauchy problems, respectively. The Cauchy problems investigated in this study have been solved using a uniform distribution of both the boundary collocation points $\mathbf{x}^i, i = 1, \dots, N$, and the source points $\mathbf{y}^j, j = 1, \dots, M$, with the mention that the latter were located on the boundary of the cube $\bar{\Omega} = (-R, R)^3 \subset \mathbb{R}^3$, where $R > 0$ was chosen such that $\bar{\Omega} \subset \tilde{\Omega}$, i.e. $R > 0.5$. Furthermore, the number of boundary collocation points on the overspecified boundary Γ_1 was set to $N = 600 \times \text{meas}(\Gamma_1)/\text{meas}(\Gamma)$ for both examples considered. More precisely, we consider $N^{(j)} = 100$ collocation points uniformly distributed on each part $\Gamma^{(j)} \subset \Gamma_1$, so that $N = 5N^{(j)}, N = 3N^{(j)}$ and $N = N^{(j)}$ in the case of under-, equally- and over-determined Cauchy data, respectively.

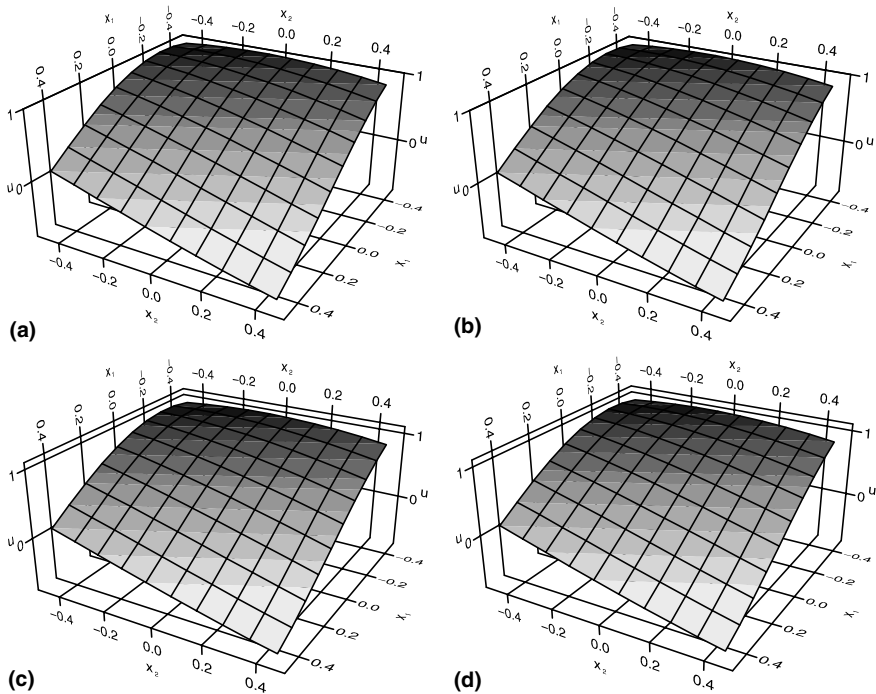


Fig. 2. (a) The analytical $u^{(\text{an})}$ and the numerical $u^{(\lambda)}$ acoustical fields, retrieved on the underspecified boundary $\Gamma^{(6)} = \Gamma_2$ with $M = 600$ source points, $N = 500$ boundary collocation points, $R = 5.0$, $\lambda = \lambda_{\text{opt}}$ and various levels of noise added into the acoustical field $u|_{\Gamma_1}$, namely (b) $p_u = 1\%$, (c) $p_u = 3\%$ and (d) $p_u = 5\%$, for Example 1(i).

4.1. Stability of the method

In order to investigate the stability of the MFS, the acoustical field $u|_{\Gamma_1} = u^{(an)}|_{\Gamma_1}$, has been perturbed as $\tilde{u} = u + \delta u$, where δu is a Gaussian random variable with mean zero and standard deviation $\sigma = \max_{\Gamma_1} |u|(p_u/100)$, generated by the NAG subroutine G05DDF, and $p_u\%$ is the percentage of additive noise included in the input data $u|_{\Gamma_1}$ in order to simulate the inherent measurement errors.

Fig. 1(a) presents the L-curves obtained for the Cauchy problem given by Example 1(iii), i.e. over-determined Cauchy data, using the zeroth-order Tikhonov regularization method, i.e. $s = 1$ in expression (12), to solve the MFS system of Eqs. (9), $M = 150$ source points, $R = 5.0$ and with various levels of noise. From this figure it can be seen that for each amount of noise considered, the “corner” of the corresponding L-curve can be clearly determined and this

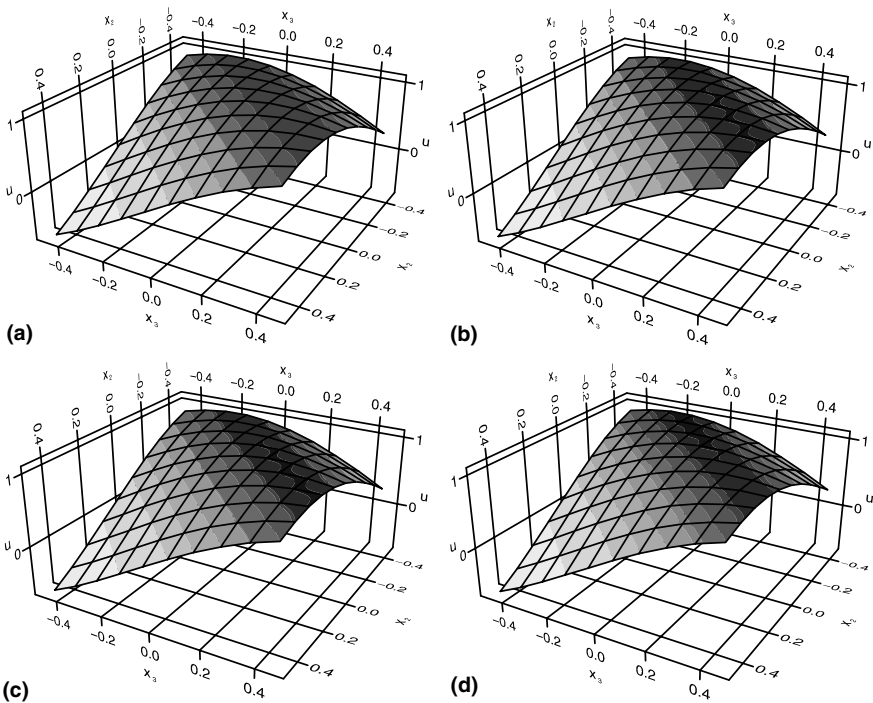


Fig. 3. (a) The analytical $u^{(an)}$ and the numerical $u^{(\lambda)}$ acoustical fields, retrieved on the underspecified boundary $\Gamma^{(4)} \subset \Gamma_2$ with $M = 600$ source points, $N = 300$ boundary collocation points, $R = 5.0$, $\lambda = \lambda_{opt}$ and various levels of noise added into the acoustical field $u|_{\Gamma_1}$, namely (b) $p_u = 1\%$, (c) $p_u = 3\%$ and (d) $p_u = 5\%$, for Example 1(ii).

gives $\lambda = \lambda_{\text{opt}} = 1.0 \times 10^{-4}$ and $\lambda = \lambda_{\text{opt}} = 1.0 \times 10^{-3}$ for $p_u = 1$ and $p_u \in \{3, 5\}$, respectively.

In order to analyse the accuracy of the numerical results obtained, we introduce the errors e_u and e_v given by

$$\begin{aligned}
 e_u(\lambda) &= \frac{1}{L} \left\{ \sum_{l=1}^L \|u^{(\text{an})}(\mathbf{x}^l) - u^{(\lambda)}(\mathbf{x}^l)\|_2^2 \right\}^{1/2}, \\
 e_v(\lambda) &= \frac{1}{L} \left\{ \sum_{l=1}^L \|v^{(\text{an})}(\mathbf{x}^l) - v^{(\lambda)}(\mathbf{x}^l)\|_2^2 \right\}^{1/2},
 \end{aligned}
 \tag{16}$$

where \mathbf{x}^l , $l = 1, \dots, L$, are $L = 600 \times \text{meas}(\Gamma_2)/\text{meas}(\Gamma)$ uniformly distributed points on the underspecified boundary Γ_2 , $u^{(\text{an})}$ and $v^{(\text{an})}$ are the analytical acoustical field and normal velocity of the sound on Γ_2 , respectively, and $u^{(\lambda)}$ and $v^{(\lambda)}$ are the acoustical field and normal velocity of the sound on Γ_2 , respectively, obtained for the value λ of the regularization parameter. Fig. 1(b) and

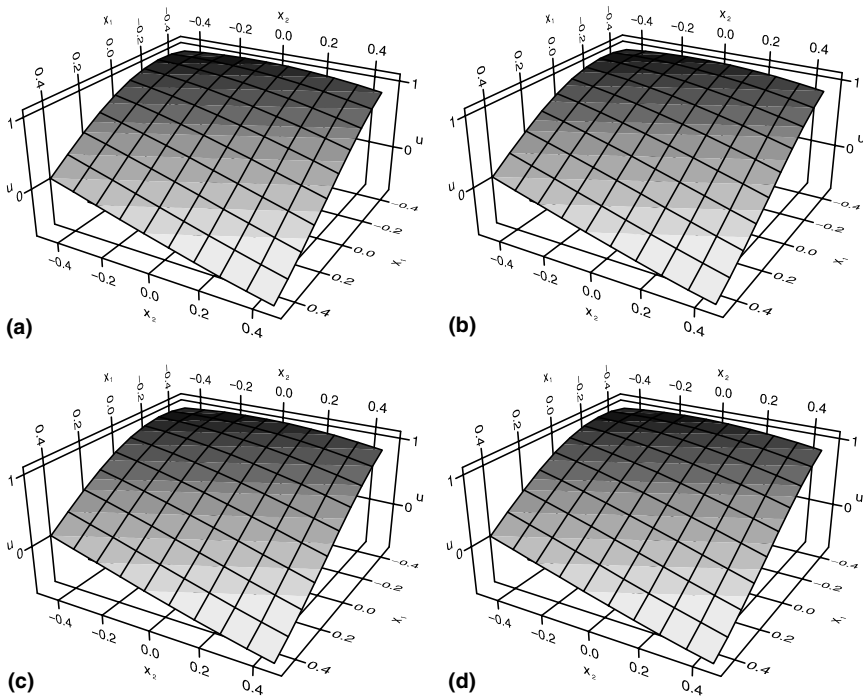


Fig. 4. (a) The analytical $u^{(\text{an})}$ and the numerical $u^{(\lambda)}$ acoustical fields, retrieved on the underspecified boundary $\Gamma^{(6)} \subset \Gamma_2$ with $M = 150$ source points, $N = 100$ boundary collocation points, $R = 5.0$, $\lambda = \lambda_{\text{opt}}$ and various levels of noise added into the acoustical field $u|_{\Gamma_1}$, namely (b) $p_u = 1\%$, (c) $p_u = 3\%$ and (d) $p_u = 5\%$, for Example 1(iii).

(c) illustrate the accuracy errors e_u and e_v , respectively, given by relation (16), as functions of the regularization parameter λ , obtained with various levels of noise added into the input acoustical field data $u|_{\Gamma_1}$ for the Cauchy problem given by Example 1(iii). From these figures it can be seen that both errors e_u and e_v decrease as the level of noise p_u added into the input acoustical field data decreases for all the regularization parameters λ and $e_u < e_v$ for all the regularization parameters λ and a fixed amount p_u of noise added into the input acoustical field data, i.e. the numerical results obtained for the acoustical field are more accurate than those retrieved for the normal velocity of the sound on the underspecified boundary Γ_2 . Furthermore, by comparing Fig. 1(a)–(c), it can be seen, for various levels of noise, that the “corner” of the L-curve occurs at about the same value of the regularization parameter λ where the minimum in the accuracy errors e_u and e_v is attained. Hence the choice of the optimal regularization parameter λ_{opt} according to the L-curve criterion is fully justified. Similar results have been obtained for the Cauchy problems given by Examples 1(i) and (ii) and 2(i)–(iii) and therefore they are not presented here.

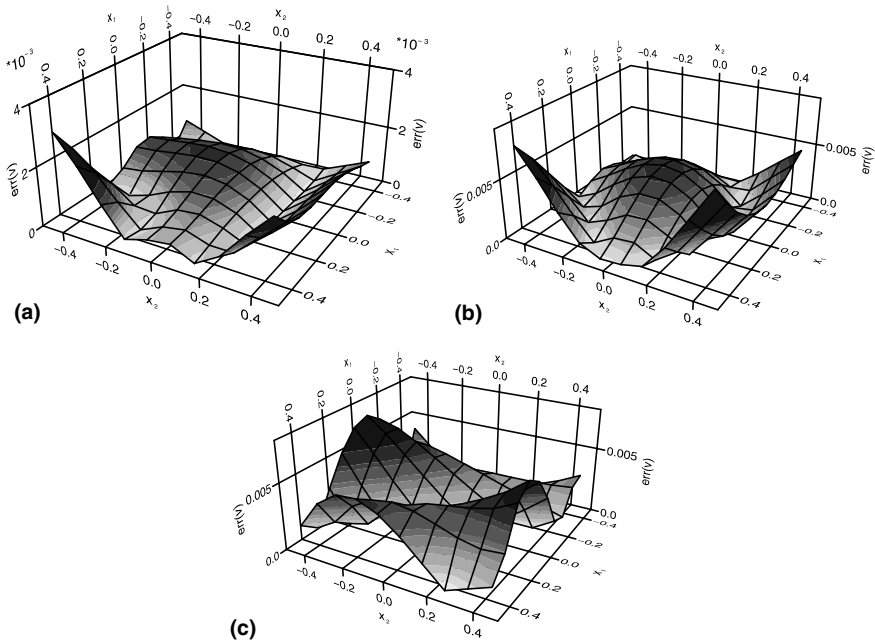


Fig. 5. The normalised error $\text{err}(v(x))$ retrieved on the underspecified boundary $\Gamma^{(6)} = \Gamma_2$ with $M = 600$ source points, $N = 500$ boundary collocation points, $R = 5.0$, $\lambda = \lambda_{\text{opt}}$ and various levels of noise added into the acoustical field $u|_{\Gamma_1}$, namely (a) $p_u = 1\%$, (b) $p_u = 3\%$ and (c) $p_u = 5\%$, for Example 1(i).

Figs. 2–4 illustrate the analytical and the numerical results for the acoustical field u obtained on parts of the underspecified boundary Γ_2 using the optimal regularization parameter $\lambda = \lambda_{\text{opt}}$ chosen according to the L-curve criterion and various levels of noise added into the input acoustical field data $u|_{\Gamma_1}$, namely $p_u \in \{1, 3, 5\}$, for the Cauchy problems given by Examples 1(i)–(iii), respectively. Although not presented here, it should be noted that similar results have been obtained for the normal velocity of the sound v in the case of Examples 1(i)–(iii), as well as for the Examples 2(i)–(iii).

The stability of the numerical method employed can be described quantitatively by defining the normalised errors

$$\begin{aligned} \text{err}(u(\mathbf{x})) &= \frac{|u^{(\text{an})}(\mathbf{x}) - u^{(\lambda)}(\mathbf{x})|}{\mathbf{y} \in \tilde{\Gamma} \max |u^{(\text{an})}(\mathbf{y})|}, \\ \text{err}(v(\mathbf{x})) &= \frac{|v^{(\text{an})}(\mathbf{x}) - v^{(\lambda)}(\mathbf{x})|}{\mathbf{y} \in \tilde{\Gamma} \max |v^{(\text{an})}(\mathbf{y})|}, \end{aligned} \tag{17}$$

for the acoustical field and the normal velocity of the sound, respectively, where $\tilde{\Gamma}$ denotes the set of boundary collocation points. It is important to

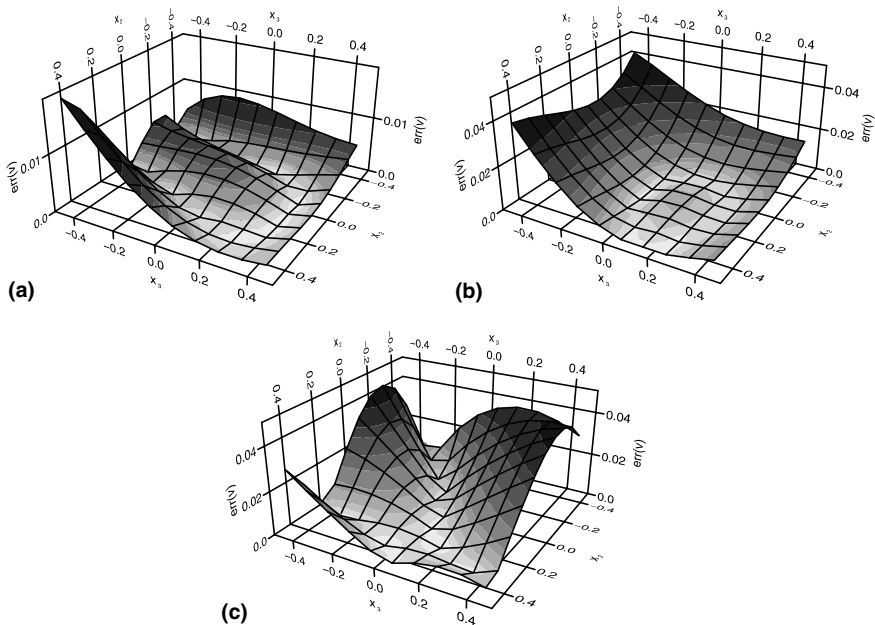


Fig. 6. The normalised error $\text{err}(v(\mathbf{x}))$ retrieved on the underspecified boundary $\Gamma^{(4)} \subset \Gamma_2$ with $M = 600$ source points, $N = 300$ boundary collocation points, $R = 5.0$, $\lambda = \lambda_{\text{opt}}$ and various levels of noise added into the acoustical field $u|_{\Gamma_1}$, namely (a) $p_u = 1\%$, (b) $p_u = 3\%$ and (c) $p_u = 5\%$, for Example 1(ii).

stress out that on using the normalised errors defined by relation (17), divisions by zero and very high errors at points where the acoustical field and/or the normal velocity of the sound have relatively small values are avoided. Figs. 5–7 present the normalised error $\text{err}(v(\mathbf{x}))$ obtained on the underspecified boundaries $\Gamma^{(6)} = \Gamma_2$, $\Gamma^{(4)} \subset \Gamma_2$ and $\Gamma^{(6)} \subset \Gamma_2$ with $p_u \in \{1, 3, 5\}$ for the Cauchy problem given by Examples 1(i)–(iii), respectively. Similar results have been obtained for the normalised error $\text{err}(u(\mathbf{x}))$, as well as for both normalised errors defined in Eq. (17) in the case of Examples 2(i)–(iii), and therefore they are not illustrated. From Figs. 1–7, we can conclude that the MFS, in conjunction with the Tikhonov zeroth-order regularization method and the L-curve criterion, is a stable numerical method with respect to decreasing the amount of noise added into the input Cauchy data.

4.2. Convergence and accuracy of the method

Although not illustrated, it is reported that the convergence of the numerical solutions for the acoustical field and the normal velocity of the sound on the

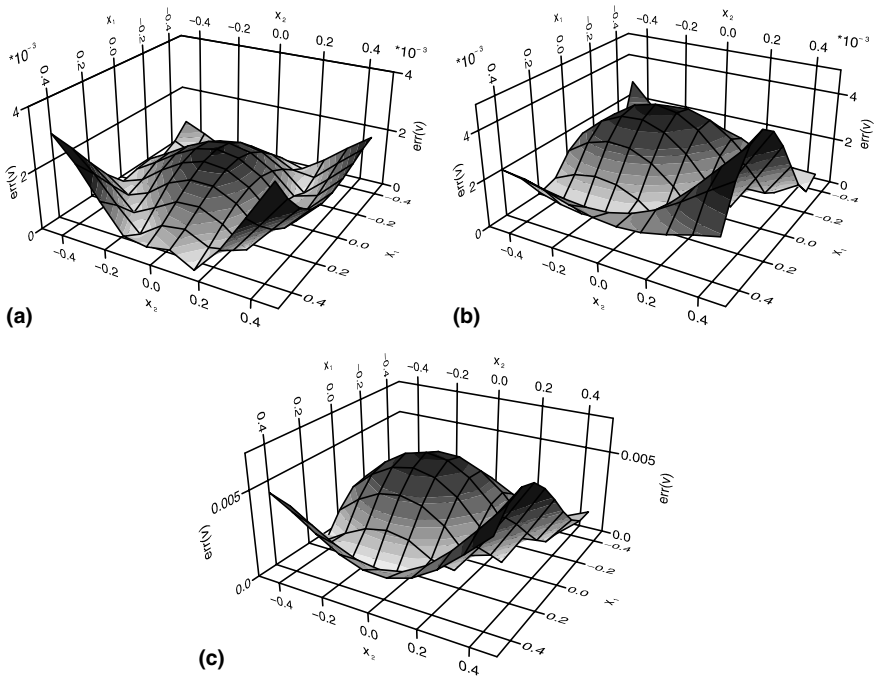


Fig. 7. The normalised error $\text{err}(v(\mathbf{x}))$ retrieved on the underspecified boundary $\Gamma^{(6)} \subset \Gamma_2$ with $M = 150$ source points, $N = 100$ boundary collocation points, $R = 5.0$, $\lambda = \lambda_{\text{opt}}$ and various levels of noise added into the acoustical field $u|_{\Gamma_1}$, namely (a) $p_u = 1\%$, (b) $p_u = 3\%$ and (c) $p_u = 5\%$, for Example 1(iii).

underspecified boundary Γ_2 towards their analytical solutions, respectively, as M or R increases, has been obtained when $p_u = 0$ for all the examples considered in this study. In order to investigate the influence of the number M of source points on the accuracy and stability of the numerical solutions for the acoustical field and the normal velocity of the sound on the underspecified boundary Γ_2 , we set $N = 600 \times \text{meas}(\Gamma_1)/\text{meas}(\Gamma)$, $R = 5.0$ and $p_u = 5$ for the Example 2. In Fig. 8(a)–(b) we present the accuracy error e_u for the Examples 2(i)–(iii), respectively, as a function of the number M of source points, obtained using $\lambda = \lambda_{\text{opt}}$ given by the L-curve criterion. It can be seen from these figures

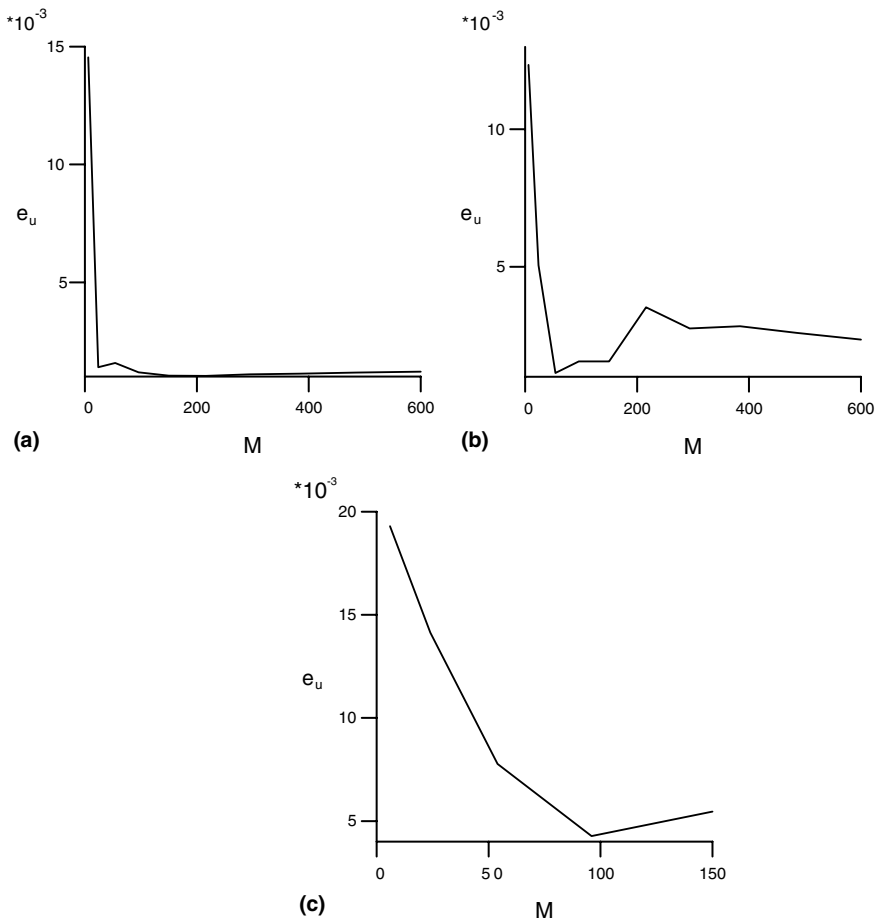


Fig. 8. The accuracy error e_u , as a function of the number M of source points, obtained with $N = 600 \times \text{meas}(\Gamma_1)/\text{meas}(\Gamma)$ boundary collocation points, $R = 5.0$, $\lambda = \lambda_{\text{opt}}$ and $p_u = 5\%$, for (a) Example 2(i), (b) Example 2(ii) and (c) Example 2(iii).

that the accuracy error e_u tends to zero as the number M of source points increases and, in addition, this error does not decrease substantially for $M \geq 24$. These results indicate the fact that the MFS in conjunction with the zeroth-order Tikhonov regularization method provides accurate and convergent numerical solutions with respect to increasing the number of source points, with the mention that a small number of source points is required in order for a good accuracy of the numerical acoustical field and normal velocity of the sound on the boundary Γ_2 to be achieved.

Next, we analyse the convergence of the numerical method proposed with respect to the position of the source points. To do so, we set

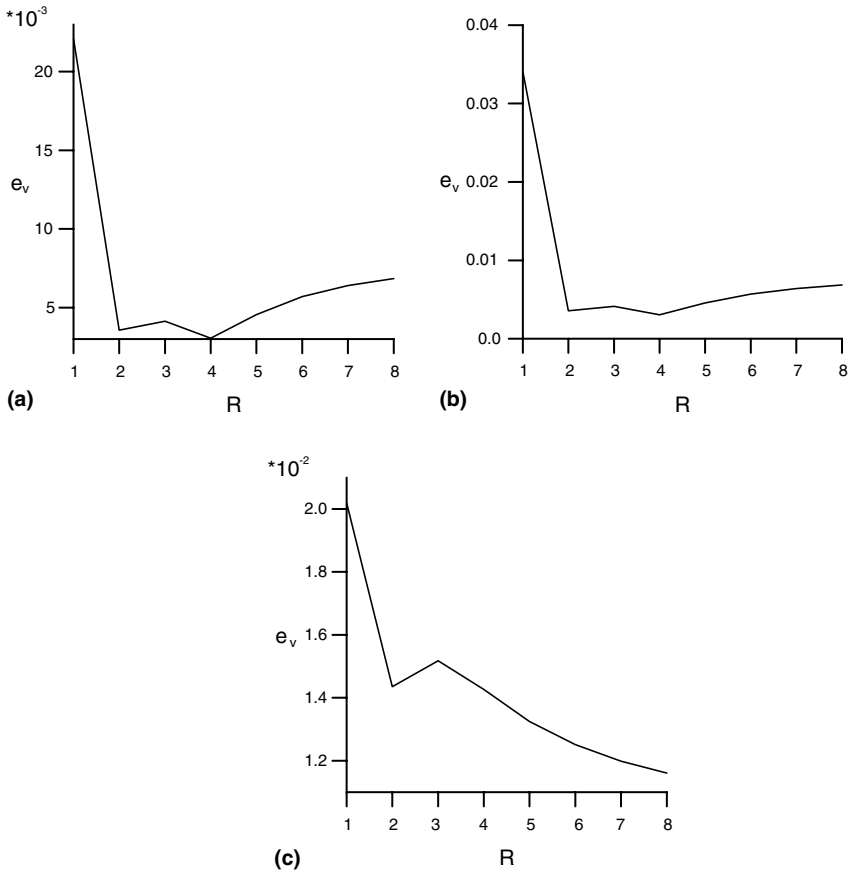


Fig. 9. The accuracy error e_v , as a function of the distance R between the source points and the boundary Γ of the solution domain Ω , obtained with $N = 600 \times \text{meas}(\Gamma_1)/\text{meas}(\Gamma)$ boundary collocation points, $\lambda = \lambda_{\text{opt}}$ and $p_u = 5\%$, for (a) Example 2(i), (b) Example 2(ii) and (c) Example 2(iii).

$N = 600 \times \text{meas}(\Gamma_1)/\text{meas}(\Gamma)$, $p_u = 5$, $M = 600$ for Examples 2(i) and (ii), and $M = 150$ for the Cauchy problem given by Example 2(iii), while at the same time varying the radius R . Fig. 9(a)–(c) illustrate the accuracy error e_v for the Examples 2(i)–(iii), respectively, as functions of R , obtained using $\lambda = \lambda_{\text{opt}}$ given by the L-curve criterion. From these figures it can be seen that the larger is the distance from the source points to the boundary Γ of the solution domain Ω , i.e. the larger is R , the better the accuracy in the numerical normal velocity of the sound. It should be noted that the value $R = 4.0$ was found to be sufficiently large such that any further increase in this distance between the source points and the boundary Γ did not significantly improve the accuracy of the numerical results for the Examples 2(i)–(iii). Although not presented here, it is reported that similar results have been obtained for all examples analysed in this study and hence we can conclude that the numerical method proposed is convergent with respect to increasing the number of source points and the distance between the source points and the boundary of the solution domain.

5. Conclusions

In this paper, the Cauchy problem associated with three-dimensional Helmholtz-type equations has been investigated by employing the MFS. The resulting ill-conditioned system of linear algebraic equations has been regularized by using the zeroth-order Tikhonov regularization method, while the choice of the optimal regularization parameter was based on the L-curve criterion. Two benchmark examples involving both the Helmholtz and the modified Helmholtz equations in a piecewise smooth geometry for under-, equally- and over-specified Cauchy problems have been analysed. The numerical results obtained show that the proposed method is convergent with respect to increasing the number of source points and the distance from the source points to the boundary of the solution domain and stable with respect to decreasing the amount of noise added into the input data. Moreover, the method is efficient and easy to adapt to three-dimensional Cauchy problems associated with Helmholtz-type equations in more complex and irregular domains, but these investigations are deferred to future work.

Acknowledgements

L. Marin would like to acknowledge the financial support received from the EPSRC. The author would also like to thank Dr. L. Elliott, Prof. D.B. Ingham and Dr. D. Lesnic from the Department of Applied Mathematics at the University of Leeds for all their encouragement in performing this research work.

References

- [1] V.D. Kupradze, M.A. Aleksidze, The method of functional equations for the approximate solution of certain boundary value problems, *USSR. Comp. Math. Math. Phys.* 4 (1964) 82–126.
- [2] R. Mathon, R.L. Johnston, The approximate solution of elliptic boundary value problems by fundamental solutions, *SIAM J. Numer. Anal.* 14 (1977) 638–650.
- [3] G. Fairweather, A. Karageorghis, The method of fundamental solutions for elliptic boundary value problems, *Adv. Comput. Math.* 9 (1998) 69–95.
- [4] K. Balakrishnan, P.A. Ramachandran, A particular solution Trefftz method for non-linear Poisson problems in heat and mass transfer, *J. Comput. Phys.* 150 (1999) 239–267.
- [5] M.A. Golberg, C.S. Chen, *Discrete projection methods for integral equations*, Computational Mechanics Publications, Southampton, 1996.
- [6] M.A. Golberg, C.S. Chen, The method of fundamental solutions for potential, Helmholtz and diffusion problems, in: M.A. Golberg (Ed.), *Boundary Integral Methods: Numerical and Mathematical Aspects*, WIT Press and Computational Mechanics Publications, Boston, 1999, pp. 105–176.
- [7] A. Karageorghis, G. Fairweather, The method of fundamental solutions for the numerical solution of the biharmonic equation, *J. Comput. Phys.* 69 (1987) 434–459.
- [8] A. Poullikkas, A. Karageorghis, G. Georgiou, Methods of fundamental solutions for harmonic and biharmonic boundary value problems, *Comput. Mech.* 21 (1998) 416–423.
- [9] A. Poullikkas, A. Karageorghis, G. Georgiou, The method of fundamental solutions for inhomogeneous elliptic problems, *Comput. Mech.* 22 (1998) 100–107.
- [10] A. Poullikkas, A. Karageorghis, G. Georgiou, The numerical solution of three-dimensional Signorini problems with the method of fundamental solutions, *Eng. Anal. Bound. Elem.* 25 (2001) 221–227.
- [11] A. Karageorghis, G. Fairweather, The method of fundamental solutions for axisymmetric elasticity problems, *Comput. Mech.* 25 (2000) 524–532.
- [12] J.A. Berger, A. Karageorghis, The method of fundamental solutions for heat conduction in layered materials, *Int. J. Num. Meth. Eng.* 45 (1999) 1681–1694.
- [13] J.A. Berger, A. Karageorghis, The method of fundamental solutions for layered elastic materials, *Eng. Anal. Bound. Elem.* 25 (2001) 877–886.
- [14] A. Karageorghis, The method of fundamental solutions for the calculation of the eigenvalues of the Helmholtz equation, *Appl. Math. Lett.* 14 (2001) 837–842.
- [15] A. Poullikkas, A. Karageorghis, G. Georgiou, The numerical solution for three-dimensional elastostatics problems, *Comput. Struct.* 80 (2002) 365–370.
- [16] P.A. Ramachandran, Method of fundamental solutions: Singular value decomposition analysis, *Commun. J. Numer. Meth. Eng.* 18 (2002) 789–801.
- [17] K. Balakrishnan, R. Sureshkumar, P.A. Ramachandran, An operator splitting-radial basis function method for the solution of transient nonlinear Poisson problems, *Comput. Math. Appl.* 43 (2001) 289–304.
- [18] D.E. Beskos, *Boundary element method in dynamic analysis: Part II (1986–1996)*, *ASME Appl. Mech. Rev.* 50 (1997) 149–197.
- [19] J.T. Chen, F.C. Wong, Dual formulation of multiple reciprocity method for the acoustic mode of a cavity with a thin partition, *J. Sound Vib.* 217 (1998) 75–95.
- [20] I. Harari, P.E. Barbone, M. Slavutin, R. Shalom, Boundary infinite elements for the Helmholtz equation in exterior domains, *Int. J. Numer. Meth. Eng.* 41 (1998) 1105–1131.
- [21] W.S. Hall, X.Q. Mao, A boundary element investigation of irregular frequencies in electromagnetic scattering, *Eng. Anal. Bound. Elem.* 16 (1995) 245–252.

- [22] Y. Niwa, S. Kobayashi, M. Kitahara, Determination of eigenvalue by boundary element method, in: P.K. Banerjee, R. Shaw (Eds.), *Development in Boundary Element Methods*, Applied Science Publisher, New York, 1982, Chapter 7.
- [23] A.J. Nowak, C.A. Brebbia, Solving Helmholtz equation by boundary elements using multiple reciprocity method, in: C.M. Calomagnano, C.A. Brebbia (Eds.), *Computer Experiment in Fluid Flow*, CMP/Springer Verlag, Berlin, 1989, pp. 265–270.
- [24] J.P. Agnantiaris, D. Polyzer, D. Beskos, Three-dimensional structural vibration analysis by the dual reciprocity BEM, *Comput. Mech.* 21 (1998) 372–381.
- [25] J. Hadamard, *Lectures on Cauchy problem in linear partial differential equations*, Oxford University Press, London, 1923.
- [26] M.R. Bai, Application of BEM-based acoustic holography to radiation analysis of sound sources with arbitrarily shaped geometries, *J. Acoust. Soc. Am.* 92 (1992) 533–549.
- [27] B.K. Kim, J.G. Ih, On the reconstruction of the vibro-acoustic field over the surface enclosing an interior space using the boundary element method, *J. Acoust. Soc. Am.* 100 (1996) 3003–3016.
- [28] Z. Wang, S.R. Wu, Helmholtz equation-least-squares method for reconstructing the acoustic pressure field, *J. Acoust. Soc. Am.* 102 (1997) 2020–2032.
- [29] S.R. Wu, J. Yu, Application of BEM-based acoustic holography to radiation analysis of sound sources with arbitrarily shaped geometries, *J. Acoust. Soc. Am.* 104 (1998) 2054–2060.
- [30] T. DeLillo, V. Isakov, N. Valdivia, L. Wang, The detection of the source of acoustical noise in two dimensions, *SIAM J. Appl. Math.* 61 (2001) 2104–2121.
- [31] T. DeLillo, V. Isakov, N. Valdivia, L. Wang, The detection of surface vibrations from interior acoustical pressure, *Inverse Probl.* 19 (2003) 507–524.
- [32] L. Marin, L. Elliott, P.J. Heggs, D.B. Ingham, D. Lesnic, X. Wen, An alternating iterative algorithm for the Cauchy problem associated to the Helmholtz equation, *Comput. Meth. Appl. Mech. Eng.* 192 (2003) 709–722.
- [33] L. Marin, L. Elliott, P.J. Heggs, D.B. Ingham, D. Lesnic, X. Wen, Conjugate gradient-boundary element solution to the Cauchy problem for Helmholtz-type equations, *Comput. Mech.* 31 (2003) 367–377.
- [34] A.N. Tikhonov, V.Y. Arsenin, *Methods for Solving Ill-Posed Problems*, Nauka, Moscow, 1986.
- [35] P.C. Hansen, The L-curve and its use in the numerical treatment of inverse problems, in: P. Johnston (Ed.), *Computational Inverse Problems in Electrocardiology*, WIT Press, Southampton, 2001, pp. 119–142.
- [36] G. Chen, J. Zhou, *Boundary Element Methods*, Academic Press, London, 1992.
- [37] P.C. Hansen, *Rank-Deficient and Discrete Ill-Posed Problems: Numerical Aspects of Linear Inversion*, SIAM, Philadelphia, 1998.
- [38] A.N. Tikhonov, A.S. Leonov, A.G. Yagola, *Nonlinear Ill-Posed Problems*, Chapman & Hall, London, 1998.
- [39] M. Hanke, Limitations of the L-curve method in ill-posed problems, *BIT* 36 (1996) 287–301.
- [40] C.R. Vogel, Non-convergence of the L-curve regularization parameter selection method, *Inverse Probl.* 12 (1996) 535–547.